Multi-Static Dispersed Swarm Configurations for Synthetic Aperture Radar Imaging

Josef Mittermayer, Gerhard Krieger, *Fellow, IEEE*, and Michelangelo Villano, *Senior Member, IEEE*

***Abstract*— The paper proposes a systematic derivation and description of Dispersed SAR for uniform inter-satellite separation, points out some of its major challenges, i.e., gapless sampling and power consumption, and provides solutions for them. By means of a reference stripmap scenario the improvements introduced by dispersed SAR using either fixed or alternating transmit satellites are discussed. It is shown that dispersed configurations allow for both a transmit power suited for small satellites, and safe intersatellite separations.**

***Index Terms* — Synthetic Aperture Radar, Small Satellite Formation, Dispersed Configuration.**

I. Introduction

MULTISTATIC Synthetic Aperture Radar (SAR) concepts are increasingly emerging [1]-[3]. Multistatic Swarm concepts can reduce the Pulse Repetition Frequency *PRF* and by this allow for, e.g., high-resolution wide-swath imaging [1],[2],[5]-[8]. As stated in [2],[9], antenna Phase Centers (PC) or satellites can be separated by distances longer than the Synthetic Aperture (SA) sampling distance. This is a *dispersed* configuration as considered below. In two conference papers dispersed SAR with uniform inter-satellite separation was dealt with [7], [8]. While in [6] simultaneous pulse transmission from all satellites is proposed for power reduction, here we presume only one transmitting satellite at a time allowing for coherent integration of all SA samples. In [4], the relation of PC, satellite velocity and several receiving apertures is described for multiple aperture satellites. [4] also discusses PRF scenarios for uniform sampling and sampling with repeated PC that can also be applied to the fixed transmit (Tx) dispersed receive (Rx) configuration $\mathbf{C_{FD}}$ in Section II.D. Also [2] discusses $\mathbf{C_{FD}}$ under the heading *SAR Train with a Single Transmit.*

The paper at hand provides a systematic derivation for closed and dispersed configurations with both fixed and alternating Tx satellites in case of uniform inter-satellite separation. It introduces formulas or algorithms that provide a gapless SA as well as compensation for PC that may be lost in case of a Frequency Modulated Continuous Wave (FMCW) operation.

The paper shows that alternating the Tx pulse between all swarm satellites is most suitable for small satellites with limited resources, i.e., mean power. In Section V, Tx alternation by pulse is discussed briefly w.r.t. alternation by Data Take (DT).

The paper presupposes inter-satellite time and phase synchronization as well as autonomous formation flying [11] that provide a uniform sampling of the SA with residual position errors significantly smaller than the Nyquist sampling distance. There are techniques, e.g. [9], that can reconstruct uniformity in case of such small residual position errors.

II. Derivation of Dispersed SAR Configurations

The fundamental question for distributed formations is how to achieve both along-track inter-satellite separations, which are large enough to be safe, and a gapless SA sampling. This section defines a monostatic stripmap reference configuration and briefly discusses close swarm configurations in preparation to the derivation of the dispersed configurations.

A. Reference Configuration $\mathbf{C_R}$ and Overall Assumptions

A single satellite at 514 km altitude and 7611 m/s velocity V_s transmits with PRF_R. The $_R$ means "Reference" and indicates variables of $\mathbf{C_R}$. The wavelength is 0.032 m and a PRF_R of 9.687 kHz is required to properly sample 0.91 m azimuth resolution.

The start-stop approximation is made and travelling pulses are neglected. Thus, the satellite Location at pulse transmission L_{Tx} and at echo reception L_{Rx} is considered identical and identical to the Location of the effective antenna PC (L_{PC}). In Fig. 1, L_{Tx}, L_{Rx} and L_{PC} along the flight path are indicated by green and red circles and blue crosses, respectively. A series of L_{PC} is obtained with the reference PC distance a_R of 0.7856 m corresponding to the parameters in the previous paragraph. In the following, a_R serves as measure for satellite and PC locations.

$$a_R = V_S / PRF_R \tag{1}$$

A SAR train formation [2] with a number of n satellites with inter-satellite distances d is analyzed in the next sections. For $\mathbf{C_R}$ with one satellite, d_R is not applicable and n_R is one.

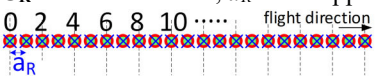

Fig. 1. Satellite location at pulse transmission (green), echo reception (red), and PC position (blue) for the reference configuration $\mathbf{C_R}$.

B. Fixed Tx / Close Swarm Rx Configuration $\mathbf{C_{FC}}$

Fig. 2 left shows a $\mathbf{C_{FC}}$ with $n = 5$. It is a close swarm of Rx satellites, where only one of them (and always the same) is also transmitting. The *PRF* is presupposed to be adjusted to a_R in the following, cf. (1). In a close swarm, d is twice a_R. In the following, a normalization by a_R is annotated by a circumflex.

$$d = 2 \cdot a_R \;\; \Rightarrow \;\; \hat{d} = d / a_R = 2 \tag{2}$$

The Tx/Rx satellite is the outer left, but principally it can be any satellite. The first line indicates the swarm location as well as L_{Tx}, L_{Rx}, and L_{PC} at time of the first pulse transmission, the second at second transmission etc., as illustrated by the vertical axis on the left. A L_{PC} is always at the middle position between the corresponding L_{Tx} and L_{Rx}. The swarm advancement between two consecutive Tx pulses is p, so for $\mathbf{C_{FC}}$, $\hat{p}_{FC}$ is marked in the figure. $\mathbf{C_{FC}}$ provides pulse-sequentially the same gapless L_{PC} series as $\mathbf{C_R}$ and is characterized by:

$$\hat{d}_{FC} = 2 \;\; ; \hat{p}_{FC} = n \;\; ; PRF_{FC} = PRF_R / n \tag{3}$$

PRF_{FC} is reduced w.r.t. $\mathbf{C_R}$ by n, e.g., [1], [2], [7]. The inter-satellite distance d_{FC} of 1.57 m is too small to be safely flown.

C. Alternating Tx / Close Swarm Rx Configuration $\mathbf{C_{AC}}$

In terms of flexibility, redundancy, and mean Tx power, it is advantageous to alternate pulse transmission between all satellites. Fig. 2 on the right shows a $\mathbf{C_{AC}}$ for a cyclical shift of the Tx satellite from pulse to pulse into flight direction.

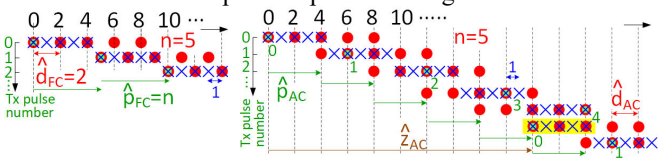

Fig. 2. (left) Fixed Tx / close swarm Rx configuration $\mathbf{C_{FC}}$ with 5 satellites. (right) Alternating Tx / close swarm Rx configuration $\mathbf{C_{AC}}$ with 5 satellites.

$\mathbf{C_{AC}}$ is characterized by (4) with z being the cycle distance that the swarm travels between two successive transmit pulses from one and the same Tx satellite.

$$\hat{d}_{AC} = 2 \quad ; \hat{p}_{AC} = n-1 \quad ; \hat{z}_{AC} = n \cdot \hat{p}_{AC} \tag{4}$$

For gapless sampling, $\hat{p}_{AC}$ needs to be by 1 smaller than n. This increases slightly the PRF w.r.t. $\mathbf{C_{FC}}$ and causes a repetition of L_{PC}, which is expressed by a PC repetition factor R_{AC}. In the figure, the PC repetition is highlighted in yellow.

$$PRF_{AC} = \frac{V_S}{p_{AC}} = \frac{V_S}{(n-1)\cdot a_R} = \frac{PRF_R}{(n-1)} \; ; R_{AC} = \frac{n \cdot n}{\hat{z}_{AC}} = \frac{n \cdot n}{n \cdot (n-1)} = \frac{n}{n-1} \tag{5}$$

R_{AC} derives from $\hat{z}_{AC}$ and the total number of L_{PC} generated in one cycle, i.e., each satellite transmits once. In Fig. 2, R_{AC} equals to 1.2. For $\hat{p}_{AC} > 1$, a gapless series of L_{PC} is only possible for a cyclical Tx pulse shift from one satellite to its neighbor into the flight direction, i.e. 1st pulse from satellite 0, 2nd pulse from satellite 1, and so on. All other sequences result in gaps if the constant PRF in (5) is used.

In a close swarm, d is always $2 \cdot a_R$ (cf. (2)), i.e. 1.57 m in the example acquisition, and too small for a safe formation. Hence, dispersed configurations are introduced in the following.

D. Fixed Tx / Dispersed Swarm Rx Configuration $\mathbf{C_{FD}}$

In a classical SAR system such as $\mathbf{C_R}$, the L_{PC} line up in the sequence of the associated transmit pulses. In a close swarm such as $\mathbf{C_{FC}}$ or $\mathbf{C_{AC}}$, the L_{PC} are obtained in successive blocks that are lined up in the Tx pulse sequence. In contrast, in a *dispersed* configuration, the L_{PC} are not obtained in the Tx pulse sequence. This is shown in Fig. 3 that shows a $\mathbf{C_{FD}}$ with $n = 5$.

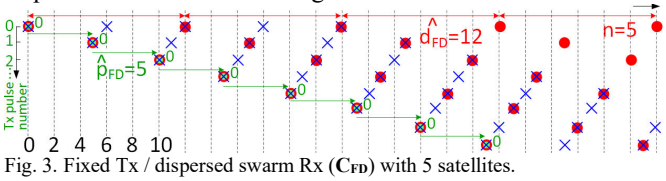

Fig. 3. Fixed Tx / dispersed swarm Rx ($\mathbf{C_{FD}}$) with 5 satellites.

The distance d is increased and the L_{PC} obtained from pulse 0 are spatially interleaved with the L_{PC} obtained from subsequent pulses. Due to this interleaving, some L_{PC} might be missing and some might be available multiple times. Based on Fig. 3, the following observations are made for dispersed configurations:

- d needs to be an even multiple of a_R, e.g., $\hat{d}_{FD} = 12$ in Fig. 3. This avoids L_{PC} in-between the reference ones.
- The formation advances by $\hat{p}_{FD}$ until a next pulse is transmitted and n PCs are obtained from that pulse. Thus, for gaplessness, $\hat{p}_{FD}$ cannot be larger than n.
- If $\hat{p}_{FD}$ equals n, there are no L_{PC} repetitions.
- To avoid systematic L_{PC} repetitions in case of $\hat{p}_{FD} < n$, $\hat{d}_{FD}$ should not be a multiple of $\hat{p}_{FD}$.
- $\hat{d}_{FD}$ can principally be as large as desired, apart from restrictions imposed by the azimuth antenna pattern.

The gaplessness condition for $\mathbf{C_{FD}}$ is derived starting from (6). The locations $\hat{L}_{Tx,FD}$, $\hat{L}_{Rx,FD}$ and $\hat{L}_{PC,FD}$ are written as a function of Tx pulse number i, with $\hat{d}_{FD}$, $\hat{p}_{FD}$ and n being parameters. A set N_{Rx} is defined, that contains the swarm satellite numbers.

$$\begin{aligned}
&\hat{L}_{Tx,FD}(i) = i \cdot \hat{p}_{FD} && ; i \in \mathbb{N}_0 \\
&\hat{L}_{Rx,FD}(i,j) = i \cdot \hat{p}_{FD} + j \cdot \hat{d}_{FD} && ; j \in N_{Rx} = \{0,1,\ldots,n-1\} \\
&\hat{L}_{PC,FD}(i,j) = \frac{\hat{L}_{Tx,FD} + \hat{L}_{Rx,FD}}{2} = i \cdot \hat{p}_{FD} + \frac{j \cdot \hat{d}_{FD}}{2} \\
&{}_{MOD}\hat{L}_{PC,FD}(j) = \hat{L}_{PC,FD}(i=0,j) \; MOD \; \hat{p}_{FD} = \left(\frac{j \cdot \hat{d}_{FD}}{2}\right) MOD \; \hat{p}_{FD}
\end{aligned} \tag{6}$$

In Fig. 3, it can be observed that if all $\hat{L}_{PC}$ from $\hat{L}_{Tx,FD}(i)$ to $\hat{L}_{Tx,FD}(i) + \hat{p}_{FD} - 1$ are obtained, gaplessness is achieved. Thus, it is sufficient to consider only the $\hat{L}_{PC}$ generated by one Tx pulse if a modulo operation is considered. In (6), the modulo operator MOD is introduced with a period of $\hat{p}_{FD}$ to define the periodic set ${}_{MOD}\hat{L}_{PC,FD}$. The preceding subscript $_{MOD}$ indicates periodicity. The condition for gaplessness for $\mathbf{C_{FC}}$ is formulated in (7) with $\{{}_{MOD}\hat{L}_{PC,FD}\}$ being the set of all ${}_{MOD}\hat{L}_{PC,FD}(j)$ for $j \in N_{Rx}$.

$$N_{RX} - \{{}_{MOD}\hat{L}_{PC,FD}\} = \{\;\} \tag{7}$$

The empty set is represented by { }. The appendix shows that this condition is fulfilled if the Greatest Common Divisor (GCD) of $\hat{d}_{FD}/2$ and $\hat{p}_{FD}$ is 1, i.e., $\hat{d}_{FD}/2$ and $\hat{p}_{FD}$ are co-prime. To avoid repeated $\hat{L}_{PC}$, $\hat{p}_{FD}$ should be set to n. In case that GCD is not 1, the following options are available (cf. Fig. 3, Fig. 4):

- Decrease $\hat{p}_{FD}$ to be not anymore equal but smaller than n. This will cause $\hat{L}_{PC}$ repetitions.
- Modify $\hat{d}_{FD}$, which changes the inter-satellite distance.
- Change slightly PRF_R. For example, if n is 13 and $\hat{d}_{FD}$ is 182, the GCD(182/2, 13) is 13. Changing PRF_R from 9.687 Hz to 9.793 kHz provides a $\hat{d}_{FD}$ of 184, and the GCD is 1.

PRF_{FD} and the repetition rate R_{FD} derive directly from $\hat{d}_{FD}$:

$$PRF_{FD} = \frac{V_S}{\hat{p}_{FD} \cdot a_R} = \frac{PRF_R}{\hat{p}_{FD}} \quad ; \text{if gap-free} \rightarrow R_{FD} = \frac{n}{\hat{p}_{FD}} \tag{8}$$

For a $\mathbf{C_{FD}}$ example with $n = 13$ and an initial $\hat{d}_{FD}$ of 182 (d_{FD} = 142 m), Fig. 4 displays the number (quantity) of acquired samples N_S at the $\hat{L}_{PC}$ locations. A N_S of 1 means the sample at $\hat{L}_{PC}$ is acquired once, a N_S of 2 means the sample is acquired two times. A N_S of 0 indicates a missing sample.

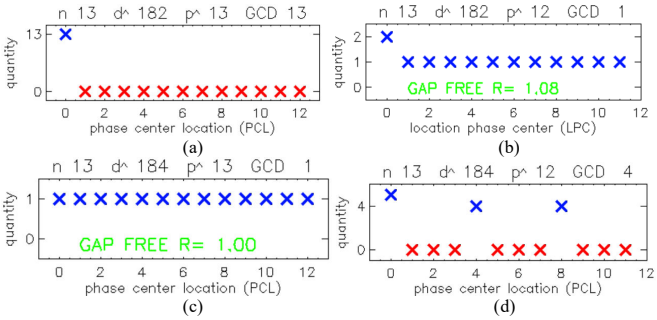

Fig. 4. $\mathbf{C_{FD}}$ examples with n=13. The quantity of each L_{PC} is provided for several combinations of $\hat{d}_{FD}$ and $\hat{p}_{FD}$. (a) The GCD is 13, $\hat{L}_{PC}$ 0 is available 13 times but all other $\hat{L}_{PC}$ are not available. (b) The formation advancement $\hat{p}_{FD}$ is decreased. Gaplessness is achieved but $\hat{L}_{PC}$ 0 is doubled. (c) The inter-satellite distance $\hat{d}_{FD}$ is increased, gaplessness is achieved without $\hat{L}_{PC}$ repetition. (d) The GCD is 4, each 4th $\hat{L}_{PC}$ is repeated. Presence of gaps.

E. Alternating Tx / Dispersed Swarm Rx Configuration $\mathbf{C_{AD}}$

$\mathbf{C_{FD}}$ provides a solution for gapless SA sampling at large inter-satellite along-track distances. In terms of mean radar Tx power, it is useful that all satellites have Tx/Rx functionality and alternate pulse transmission. Fig. 5 provides a $\mathbf{C_{AD}}$ with n = 5 and $\hat{d}_{AD}$ = 10. The following observations can be made:

- Principally, gaps may occur for alternating configurations, e.g., gaps are indicated by grey triangles in cycle 1 of Fig. 5.
- Several $\hat{L}_{PC}$ are obtained more than once. For example, these $\hat{L}_{PC}$ are indicated by yellow boxes in Fig. 5.
- After few cycles, e.g., from cycle 3 on in Fig. 5, the PC acquisition is in a steady state. All $\hat{L}_{PC}$ from pulses of previous cycles are available additionally to the ones of the current cycle. We define such a cycle as *Steady Cycle.*
- In steady cycles, the $\hat{L}_{PC}$-pattern repeats, e.g., in Fig. 5, this can be verified at the beginning of cycle 4, that is, apart from being shifted by $\hat{z}_{AD}$, identical to the beginning of cycle 3.
- A steady cycle $\hat{L}_{PC}$-pattern can be obtained from the first *n* pulses, i.e. each satellite transmits once, if the $\hat{L}_{PC}$ outside the cycle are cyclically shifted into the cycle. This can be done by the MOD operator corresponding to a period of $\hat{z}_{AD}$.

In (9), satellite and phase center locations $\hat{L}_{Tx,AD}$, $\hat{L}_{Rx,AD}$ and $\hat{L}_{PC,AD}$ are functions of Tx pulse number *i*, with $\hat{d}_{AD}$, $\hat{p}_{AD}$ and *n* being parameters. A steady state cycle is fully described by ${}_{MOD}\hat{L}_{PC,AD}$.

$$\begin{aligned}
&\hat{L}_{Tx,AD}(i) = i\cdot\hat{p}_{AD} + (i\ MOD\ n)\cdot\hat{d}_{AD} \quad ; i\in\mathbb{N}_0\\
&\hat{L}_{Rx,AD}(i;j) = i\cdot\hat{p}_{AD} + j\cdot\hat{d}_{AD} \quad ; j\in N_{Rx}=\{0,1,\ldots,n-1\}\\
&\hat{L}_{PC,AD}(i;j) = \frac{\hat{L}_{Tx,AD}+\hat{L}_{Rx}(i;j)}{2} = i\cdot\hat{p}_{AD} + \frac{\hat{d}_{AD}}{2}\cdot\left[j+(i\ MOD\ n)\right]\\
&{}_{MOD}\hat{L}_{PC,AD}(u;j) = \left(u\cdot\hat{p}_{AD} + \frac{\hat{d}_{AD}}{2}\cdot\left[j+(u\ MOD\ n)\right]\right) MOD\ \hat{z}_{AD}; u\in N_{Rx}
\end{aligned} \tag{9}$$

For the further analysis, a matrix formulation is more practicable. We start with the generation matrix $\underline{M}_n$ in (10) that is a *n* x *n* matrix that reflects the *n* Tx pulses in a cycle and the *n* Rx satellites. The underscore indicates a matrix. From (9), the matrix $\underline{\hat{L}}_{Tx,AD}$ is obtained. It contains the first *n* Tx locations.

$$\underline{M}_n = \begin{bmatrix} 0 & 0 & \cdots & 0\\ 1 & 1 & \cdots & 1\\ \vdots & \vdots & \cdots & \vdots\\ n\text{-}1 & n\text{-}1 & \cdots & n\text{-}1\end{bmatrix};\ \underline{\hat{L}}_{TX,AD} = \underline{M}_n\cdot\left(\hat{p}_{AD}+\hat{d}_{AD}\right);\quad \underline{\hat{L}}_{TX,AD}\big|_{Fig.5} = \begin{bmatrix} 0&0&0&0&0\\ 13&13&13&13&13\\ 26&26&26&26&26\\ 39&39&39&39&39\\ 52&52&52&52&52\end{bmatrix} \tag{10}$$

$\underline{\hat{L}}_{Rx,AD}$ contains the corresponding Rx locations.

$$\underline{\hat{L}}_{RX,AD} = \underline{M}_n\cdot\hat{p}_{AD} + \underline{M}_n^T\cdot\hat{d}_{AD};\quad \underline{\hat{L}}_{RX,AD}\big|_{Fig.5} = \begin{bmatrix} 0&10&20&30&40\\ 3&13&23&33&43\\ 6&16&26&36&46\\ 9&19&29&39&49\\ 12&22&32&42&52\end{bmatrix} \tag{11}$$

The superscript ^{T} means matrix transpose. Applying MOD $\hat{z}_{AD}$ to the geometric mean of $\underline{\hat{L}}_{Tx,AD}$ and $\underline{\hat{L}}_{Rx,AD}$ results in ${}_{MOD}\underline{\hat{L}}_{PC,AD}$, which contains all the $\hat{L}_{PC}$ of a steady cycle.

$${}_{MOD}\underline{\hat{L}}_{PC,AD} = \frac{\underline{\hat{L}}_{Tx,AD}+\underline{\hat{L}}_{Rx,AD}}{2} MOD\ \hat{z}_{AD};\ {}_{MOD}\underline{\hat{L}}_{PC,AD}\big|_{Fig.5} = \begin{bmatrix} 0&5&10&15&20\\ 8&13&18&23&28\\ 16&21&26&31&36\\ 24&29&34&39&44\\ 32&37&42&47&52\end{bmatrix} MOD\ \hat{z}_{AD} = \begin{bmatrix} 0&5&10&0&5\\ 8&13&3&8&13\\ 1&6&11&1&6\\ 9&14&4&8&14\\ 2&7&12&2&7\end{bmatrix} \tag{12}$$

The first row of ${}_{MOD}\underline{\hat{L}}_{PC,AD}$ provides the $\hat{L}_{PC}$ generated by Tx pulse 0, and so on (cf. Fig. 5). By defining the sets $N_Z = \{0,1,\ldots,\hat{z}_{AD}-1\}$ and $\{{}_{MOD}\underline{\hat{L}}_{PC,AD}\}$, whereby the latter contains all $\hat{L}_{PC}$ of ${}_{MOD}\underline{\hat{L}}_{PC,AD}$, the gaplessness condition for $\mathbf{C_{AD}}$ is

$$N_Z - \{{}_{MOD}\hat{L}_{PC,AD}\} = \{\ \}. \tag{13}$$

PRF_{AD} and, in case of gaplessness, also R_{AD}, can be obtained as in (8) for $\mathbf{C_{FD}}$. In summary, for $\mathbf{C_{AD}}$ applies:

$$\hat{z}_{AD} = n\cdot\hat{p}_{AD};\ PRF_{AD} = \frac{PRF_R}{\hat{p}_{AD}};\ \text{if gapless} \rightarrow R_{AD} = \frac{n^2}{\hat{z}_{AD}} = \frac{n}{\hat{p}_{AD}} \tag{14}$$

It is not straightforward to derive a closed formulation that tells us for which values of $\hat{d}_{AD}$ and $\hat{p}_{AD}$ gaplessness is ensured (as we did for $\mathbf{C_{FD}}$). Thus, a simple algorithm is provided next that estimates gaplessness.

F. Alternating-Dispersed Algorithm for $\mathbf{C_{AD}}$

Fig. 6 on the right shows the structogram of the algorithm. The input is *n* and an examination range of even inter-satellite distances from $\hat{d}_{AD,\min}$ to $\hat{d}_{AD,\max}$. Starting with $\hat{d}_{AD,\min}$ and the maximum possible value for $\hat{p}_{AD} = n-1$, the matrix ${}_{MOD}\underline{\hat{L}}_{PC,AD}$ is generated and it is checked whether the configuration is gapless using (13). If the current loop $\hat{d}_{AD}$- $\hat{p}_{AD}$-combination is gapless, it is stored, $\hat{d}_{FD}$ increments by 2 and the $\hat{p}_{FD}$ loop starts again with *n*-1. If not, $\hat{p}_{FD}$ decrements by 1 as long as it is equal to 2, which is a trivial gapless case but with many repetitions.

Fig. 7 provides for n = 13 and the examination range for $\hat{d}_{AD}$ from 180 to 188 the $\hat{L}_{PC}$ distribution within a steady cycle for the first combinations tested by the algorithm. In Fig. 7 on the left, $\hat{d}_{AD}$ is fixed to 180, and, from top to bottom, $\hat{p}_{AD}$ is decreased from 12 down to 9, which also decrements $\hat{z}_{AD}$. None of the combinations on the left is gapless. This is also the case for all other $\hat{p}_{AD}$ values down to 3.

As shown in Fig. 6, the algorithm continues by incrementing $\hat{d}_{AD}$ to 182, and already the first $\hat{p}_{AD}$ value of 12 is gapless.

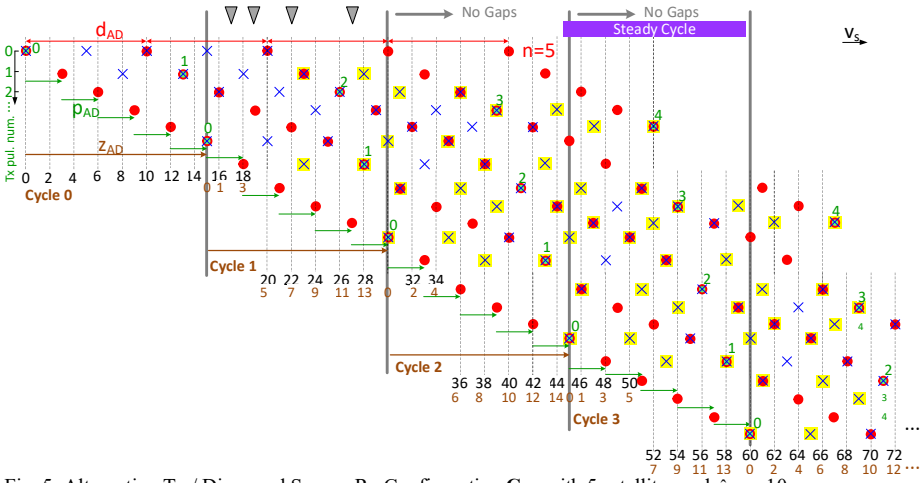

Fig. 5. Alternating Tx / Dispersed Swarm Rx Configuration $\mathbf{C_{AD}}$ with 5 satellites and $\hat{d}_{AD} = 10$.

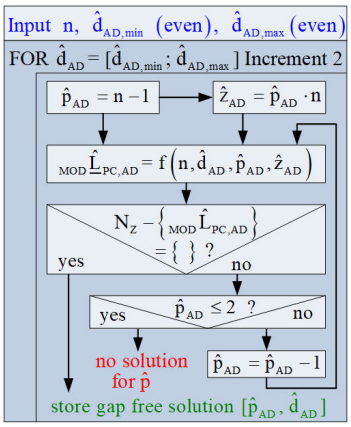

Fig. 6. Alternating-Dispersed Algorithm to test $\hat{d}_{AD}$ - $\hat{p}_{AD}$ -combinations for gaps.

Fig. 7 on top right provides the corresponding $\hat{L}_{PC}$ distribution. The other plots provide other solutions. With $\hat{d}_{AD}$ = 182 and $\hat{p}_{AD}$ = 12 the PC repetition is smallest, i.e. R_{AD} = 1.08.

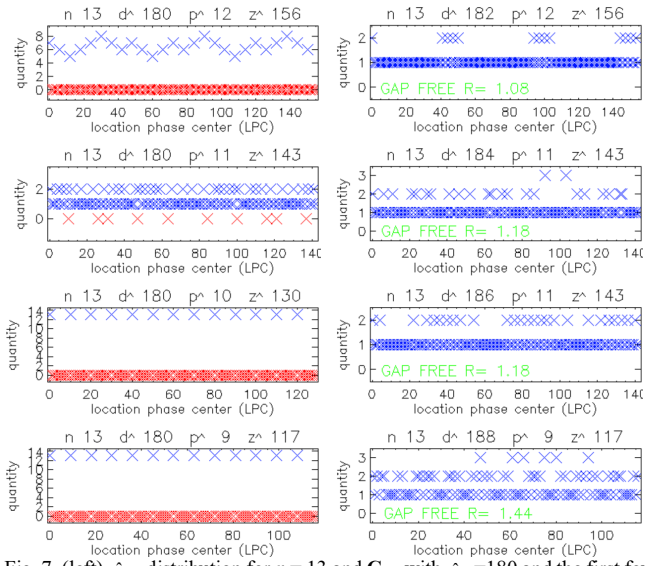

Fig. 7. (left) $\hat{L}_{PC}$ distribution for n = 13 and $\mathbf{C_{AD}}$ with $\hat{d}_{AD}$=180 and the first four $\hat{p}_{AD}$ values evaluated (from top to bottom). The quantity on the vertical axis shows how often a certain $\hat{L}_{PC}$ occurs in the $_{MOD}\hat{L}_{PC,AD}$ matrix. The condition for gaplessness is a quantity > zero for all $\hat{L}_{PC}$.

III. Power and PRF of Dispersed Configurations

This section differentiates between the whole Swarm and an Individual transmitting satellite, indicated by the subscripts S and I, respectively. If both, $\mathbf{C_{FD}}$ and $\mathbf{C_{AD}}$ are addressed, only the subscript D is used. A gapless $\hat{d}_D$ - $\hat{p}_D$ -combination is implied.

Due to the enlargement of the Rx antenna area, the swarm Rx gain increases. Consequently, *in order to obtain the same* Noise Equivalent Sigma Zero (*NESZ*) as in $\mathbf{C_R}$, the required transmit Peak Power of the Swarm ($_SPP_{req}$) reduces w.r.t. PP_R with the number of $\hat{L}_{PC}$ that are obtained from one Tx pulse (without repetitions). This decrease is n divided by R_D, cf. (15).

The required Mean Power of an individual Tx satellite ($_IMP_{req}$) for $\mathbf{C_{FD}}$ derives from the Tx duty cycle (T_{dc}). For $\mathbf{C_{AD}}$, $_IMP_{req}$ reduces further by n since all swarm satellites transmit.

$$
\begin{aligned}
&_SPP_{req,D} = PP_R \cdot \frac{R_D}{n} = PP_R \cdot \frac{n}{n \cdot \hat{p}_D} = PP_R \cdot \frac{1}{\hat{p}_D} \\
&_IMP_{req,FD} = {}_SPP_{req,D} \cdot T_{dc} \quad ; \quad _IMP_{req,AD} = {}_SPP_{req,D} \cdot T_{dc} \cdot \frac{1}{n}
\end{aligned}
\tag{15}
$$

IV. SAR System Example

A SAR system with 80 km ground Swath Width (*SW*) and ~1 m x 1 m resolution shall fulfill the requirements given in TABLE I (upper part). A single antenna cannot meet at the same time the requirements on SW and azimuth resolution due to the classical SAR limitation. For example, Section II.A and the upper table defines a reference configuration $\mathbf{C_R}$ that cannot meet the required *SW*, i.e. the PRI_R is too small to cope with the 42.5 km slant *SW* at 1 m resolution. Note, the maximum focused echo window length is $PRI \cdot (1 - 2 \cdot duty)$.

These requirements can be instead fulfilled using dispersed configurations either with fixed or alternating transmit. $\mathbf{C_R}$ is used as a starting point to derive the parameters for the $\mathbf{C_{FD}}$-$\mathbf{C_{AD}}$ comparison in the lower part of the table.

The blue part of TABLE I provides $\mathbf{C_{FD}}$ with *n, d* and *p* identical to Fig. 4 (c), an additional example with 21 satellites, and a FMCW version (cf. next section). The satellite separation is realistic, and due to the reduced swarm *PRF*, the 80 km ground *SW* can be covered. The *RASR* is sufficient. The *MP* required to provide a *NESZ* < -19 dB over the full *SW* is considered too high. The *PP* is considered high.

The green part of TABLE I contains $\mathbf{C_{AD}}$ with *n*, *d*, and *p* identical to Fig. 7 (top right), an additional 21 satellites example, and a FMCW version (cf. next section). The *SW* is covered and the *RASR* is sufficient. The *MP* per transmitting satellite is 120 W for n = 13 and 47 W for n = 21. The *PP* is considered high - on the other hand, the resolution is 1 m at 80 km *SW*. The *MP* reduction is the biggest advantage of $\mathbf{C_{AD}}$. In TABLE I, the *PP* for $\mathbf{C_{AD}}$ is slightly higher than for $\mathbf{C_{FD}}$ due to the higher R_{AD}. It causes also a reduction of the maximum *SW* limitation due to echo window timing, which nevertheless is small due to the low *PRF* and high *n*. E.g., for n = 13 and no FMCW, the timing limitation decreases from 201 km slant range for $\mathbf{C_{FD}}$ to 186 km for $\mathbf{C_{AD}}$.

One option to reduce the *PP* is to increase *n* as is shown in the 21 satellite example for $\mathbf{C_{FD}}$ and $\mathbf{C_{AD}}$ in TABLE I.

TABLE I
System and performance parameters for $\mathbf{C_R}$, $\mathbf{C_{FD}}$, and $\mathbf{C_{AD}}$

Requirements		**Reference Single Satellite C_R**	
ground width	80 km	*rect. antenna*	2.4 m x 0.2 m
slant width	**42.5 km**	*3dB-width*	0.68° x 8.05°
incidence angle	28.4°-35.6°	*processed width*	0.94° x 6.49°
resolution (az x slant)	0.9 m x 0.75 m	*az BW processed*	7750 Hz
NESZ	-19 dB	PRF_R	9687 Hz
		$PRI_R \cdot c_0/2$	15 km
Common Parameters C_R, C_{FD}, C_{AD}		*PC distance a_R*	0.7856 m
duty	0.3	*RASR*	> 8 dB
AASR	< -25 dB	*peak power (PP)*	62.6 kW
Tx bandwidth (BW)	200 MHz	*mean power (MP)*	18.8 kW

	Tx Fixed / Rx Dispersed C_{FD}			**Tx Alternating / Rx Dispersed C_{AD}**			
n	13		21	13			21
duty	FMCW	0.3	0.3	FMCW		0.3	0.3
d/a_R	182	184	184	214	194	182	210
p/a_R	12	13	21	10	7	12	19
R	1.08	1.0	1.0	1.3	1.86	1.08	1.11
PRF	807 IIz	745 IIz	461 IIz	986 IIz	1384 IIz	807 IIz	510 IIz
$PRI\ c_0/2$	186 km	201 km	325 km	155 km	108 km	186 km	294 km
z/a_R	-	-	-	130	91	156	399
lost PC	-	-	-	7	1	-	-
RASR	< -39 dB	< -44 dB	< -44 dB	<-32 dB	<-30 dB	< -39 dB	< -43 dB
PP	1566 W	4819 W	2983 W	1879 W	2684 W	5221 W	3297 W
MP	1566 W	1446 W	895 W	144 W	207 W	120 W	47 W

G. Frequency Modulated Continuous Wave (FMCW)

A FMCW operation, e.g. [10], can also be used to reduce the *PP* (same *NESZ* as $\mathbf{C_R}$). The analysis assumes that a Tx pulse on a direct path to a Rx satellites never saturates a receiver. FMCW requires highly decoupled Tx and Rx antennas. The bistatic operation provides inherently high decoupling. The $\mathbf{C_{FD}}$ can be designed to have the L_{PC} of the *unique* Tx satellite doubled (cf. Fig. 4 (b)), so during Tx the satellite can be switched off in receive. The missing L_{PC} are provided by another swarm satellite. Applying FMCW to the example $\mathbf{C_{FD}}$ of Fig. 4 (b), results in the FMCW example given in TABLE I. Here, FMCW is considered by setting the Tx duty cycle to 1.

For $\mathbf{C_{AD}}$, it is difficult to find *d*-*p*-combinations without lost L_{PC} when the transmitting satellites are switched-off in Rx. But it is possible to find some with only few lost L_{PC}. Fig. 8 shows two variants. The L_{PC} at which a satellite transmits are indicated by orange crosses. A quantity of 1 means a lost L_{PC} at transmission. A quantity of 2 means L_{PC} replacement by another satellite in receive-only. The orange text shows the count in a steady cycle of L_{PC} at transmission with quantity 0,1,2,3 or 4. Variant A loses 7 L_{PC} in a cycle length of 130, i.e., 5.4 %. Variant B loses 1 L_{PC} in a cycle length of 91, i.e., 1.1 %. TABLE I provides the according reduction in *PP* and *MP* per transmit satellite for both variants.

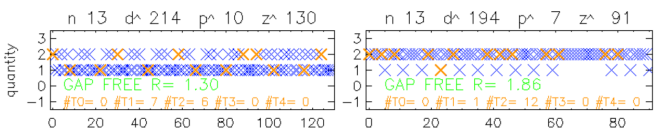

Fig. 8. (left) L_{PC} distribution for $\mathbf{C_{AD}}$ with FMCW variant A (left) and B (right). The L_{PC} at pulse transmission positions are in orange. X-axis is L_{PC}.

V. Conclusion and Discussion

The paper derived dispersed swarm configurations for multi-static SAR with fixed and alternating transmit satellite in case of uniform inter-satellite separation. For $\mathbf{C_{FD}}$, an analytical approach assures a gapless sequence of phase centers. For $\mathbf{C_{AD}}$, an algorithm searches for gapless inter-satellite distances *d* and swarm advancement p combinations.

Based on a monostatic example, the advantages of dispersed configurations were discussed. High resolution at wide swath and very low *RASR* are achievable due to the low swarm *PRF*. For $\mathbf{C_{AD}}$ and a ground *SW* of 80 km at a resolution of ~1 m, the mean power per transmit satellite is around 100 W or lower depending on the number of swarm satellites.

One could compare $\mathbf{C_{AD}}$ with a $\mathbf{C_{FD}}$ that alternates the transmit satellite from DT to DT. $\mathbf{C_{AD}}$ allows for longer DTs compared to such a configuration due to the reduced mean power per satellite when thermal and battery resources are considered, especially for small satellites.

There are at least two options to cope with a failed satellite: either to focus with the available samples in a non-optimal way, or to change the formation and re-calculate the swarm configuration by the formulas provided in the letter, i.e. new *n*, *p* and *d*, and achieve again a formation without PC gaps.

Appendix

This appendix provides the proof of the condition for gapless sampling for $\mathbf{C_{FC}}$. In (6), the locations of the PC are given by

$$\hat{L}_{PC,FD} = j \cdot \hat{d}_{FD}/2 + i \cdot \hat{p}_{FD} \quad ; j \in N_{Rx} = \{0,1,...,n-1\} \quad ; i \in \mathbb{N}_0 \tag{16}$$

The combination of values $[\hat{d}_{FD}, \hat{p}_{FD}]$ therefore allows for full sampling, if and only if each $u \in \mathbb{Z}$ can be written as

$$u = j \cdot \hat{d}_{FD}/2 + i \cdot \hat{p}_{FD} \quad ; j \in N_{Rx} \; ; i \in \mathbb{N}_0 \tag{17}$$

The combinations that satisfy the condition above are those for which the following congruence equation can be solved:

$$j \cdot \hat{d}_{FD}/2 \equiv u \; (MOD\ \hat{p}_{FD}) \quad ; j \in N_{Rx} \tag{18}$$

This linear congruence equation can be solved if and only if

$$u \equiv 0 \; (MOD\ \alpha) \quad \text{with} \quad \alpha = GCD\left(\hat{p}_{FD}, \hat{d}_{FD}/2\right) \tag{19}$$

this means if and only if $\hat{p}_{FD}$ and $\hat{d}_{FD}/2$ are co-prime.

References

[1] J. E. Winter, N. C. Anderson, "Distributed aperture implementation on the techsat 21 satellites", Proc. of Aerospace Conference, 2003.

[2] J. P. Aguttes, "The SAR train concept: Required antenna area distributed over N smaller satellites, increase of performance by N", in Proc. IGARSS, 2003.

[3] G. Krieger *et al.*, "Spaceborne bi- and multistatic SAR: potential and challenges", IEE Proc.-Radar Sonar Navig., Vol. 153, No. 3, June 2006.

[4] N. Gebert, G. Krieger, A. Moreira, "Digital Beamforming on Receive: Techniques and Optimization Strategies for High-Resolution Wide-Swath SAR Imaging", IEEE TAES, 2009.

[5] A. Renga, M. D. Graziano, M. Grasso, A. Moccia, "Evaluation of design parameters for formation flying SAR", Proc. of EUSAR, 2021.

[6] D. Giudici *et al.*, "Compact and Free-Floating Satellite MIMO SAR Formations", IEEE TGRS, 2021.

[7] J. Mittermayer, P. López-Dekker, T. Kraus, G. Krieger, "Small Satellite Dispersed SAR - an Exemplary Configuration ", Proc. of EUSAR, 2016.

[8] J. Mittermayer *et al.*, "Small Satellite Dispersed Synthetic Aperture Radar", Proc. of the ESA 4S Symposium, Valletta, Malta, 2016.

[9] G. Krieger, N. Gebert, and A. Moreira, "Unambiguous SAR signal reconstruction from nonuniform displaced phase center sampling", IEEE Geosci. Remote Sens. Lett., 2004, 1, (4), pp. 260–264.

[10] J.J. M. de Wit, "Development of an Airborne Ka-Band FM-CW Synthetic Aperture Radar" Ph.D. dissertation, Delft Univ. Technol., Delft, The Netherlands, 2005, ISBN 90-9019360-X.

[11] P. Bodin *et al.*, "The PRISMA Formation Flying Demonstrator: Overview and Conclusions from the Nominal Mission", Advances in the Astronautical Sciences, AAS Guidance and Control Conference, 2012.